

AN ATLAS OF HIGH-DISPERSION CAMERA ARTIFACTS

D. MICHAEL CRENSHAW (CSC), OTTO W. BRUEGMAN (ITMI), RITA JOHNSON
(HUGHES STX), AND MICHELE FITZURKA (CATHOLIC UNIV.)

Camera artifacts are artificial emission features that appear in every long IUE exposure. They resemble cosmic-ray hits, which can be detected in background regions by inspection of the raw images and in spectral regions by comparing more than one image of the same target. Camera artifacts are more difficult to identify than cosmic-ray hits, because they appear on every exposure that is greater than about one hour. The best way to identify camera artifacts is to study sky-background spectra, since the only "real" feature in these spectra should be geocoronal $L\alpha$ at 1216 Å in the SWP region.

A detailed study of camera artifacts in low-dispersion IUE spectra was presented by Crenshaw, Bruegman, & Norman (1990). Plots of averaged sky-background spectra were presented to aid scientists in the identification of these features in their low-dispersion spectra. The spectra were also made available through the IUEDAC procedure called "ARTIFACT".

This article presents plots of the artifacts found in high-dispersion sky-background spectra. Although these spectra were processed with IUESIPS, it is expected that the artifacts will also be present at the same approximate locations in NEWSIPS spectra, although their character may be altered somewhat (Bruegman & Crenshaw 1992). This high-dispersion atlas, together with the low-dispersion atlas in Crenshaw, Bruegman, & Norman (1990), should be useful for identifying camera artifacts in all IUE spectra.

The following figures present spectra of the artifacts for each order of each functional camera (SWP, LWP, LWR). The spectra are plotted in absolute flux units to allow direct comparison with science spectra. The noise is magnified at the ends of many orders, due to the large ripple corrections - no attempt has been made to identify artifacts in noisy regions. This effect is also present in science data, and is overcome by using data in the same wavelength region from another order.

Table 1 gives the positions and strengths of the strong high-dispersion artifacts that were detected. The *measured* positions are accurate to 0.1 - 0.2 Å for the SWP spectra and 0.2 - 0.3 Å for the LWP and LWR spectra. The *expected* positions of the artifacts in a particular science spectrum can be obtained by correcting the measured positions for the radial velocity shift that was applied to the science spectrum - this value can be found in the image header. As discussed in Crenshaw, Bruegman, & Norman (1990), the strengths of the artifacts depend on the background level and the previous history of exposures and preparation sequences. In general, the absolute flux levels can vary by a factor of ~ 3 .

This article is the only source for hard-copy plots of all of the high-dispersion sky-background spectra. More details on the reduction, analysis, and interpretation of the spectra can be found in an upcoming PASP paper (Crenshaw et al. 1996). In addition, the IUEDAC procedure ARTIFACT has been updated to return high-dispersion spectra for individual orders.

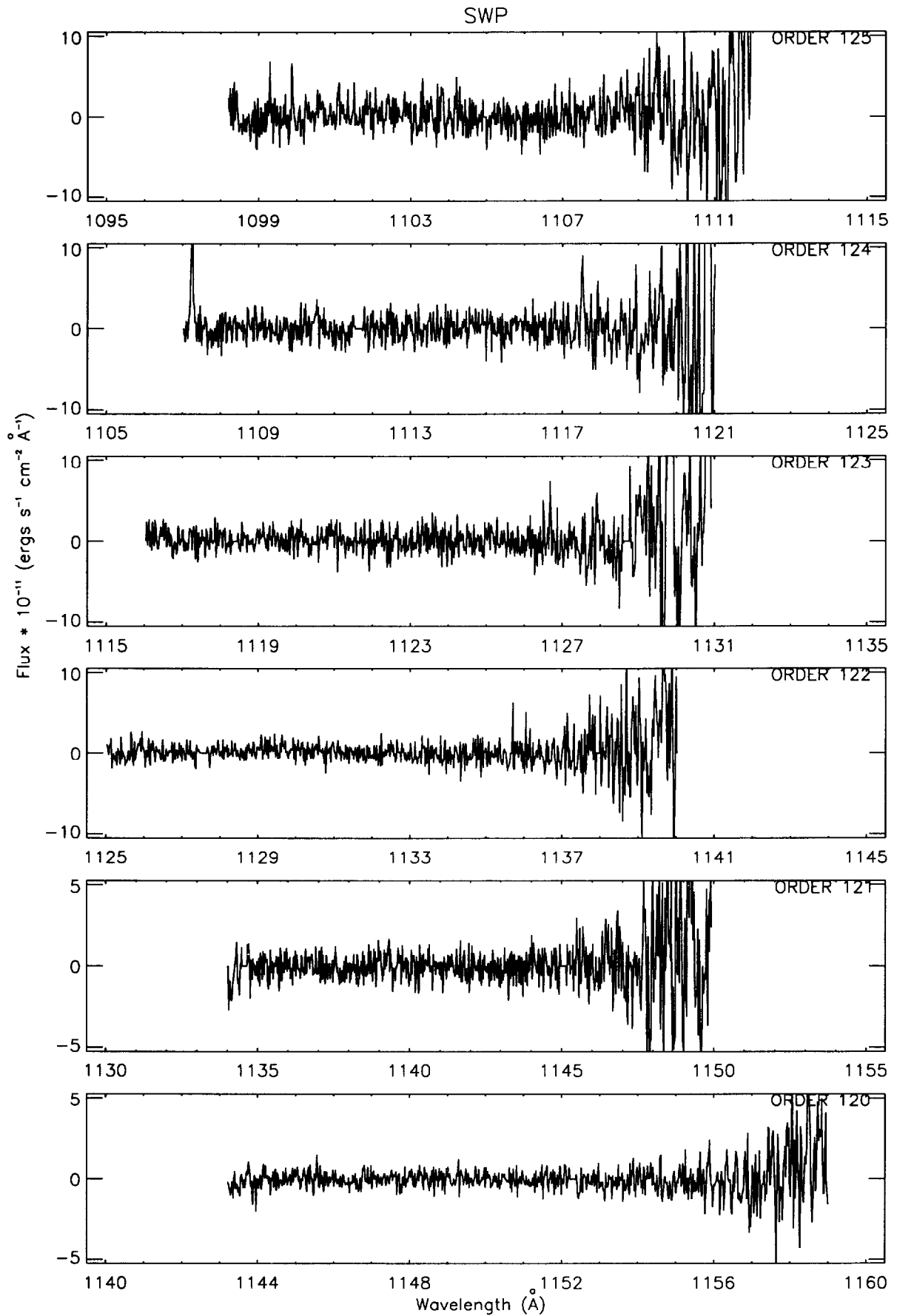
REFERENCES

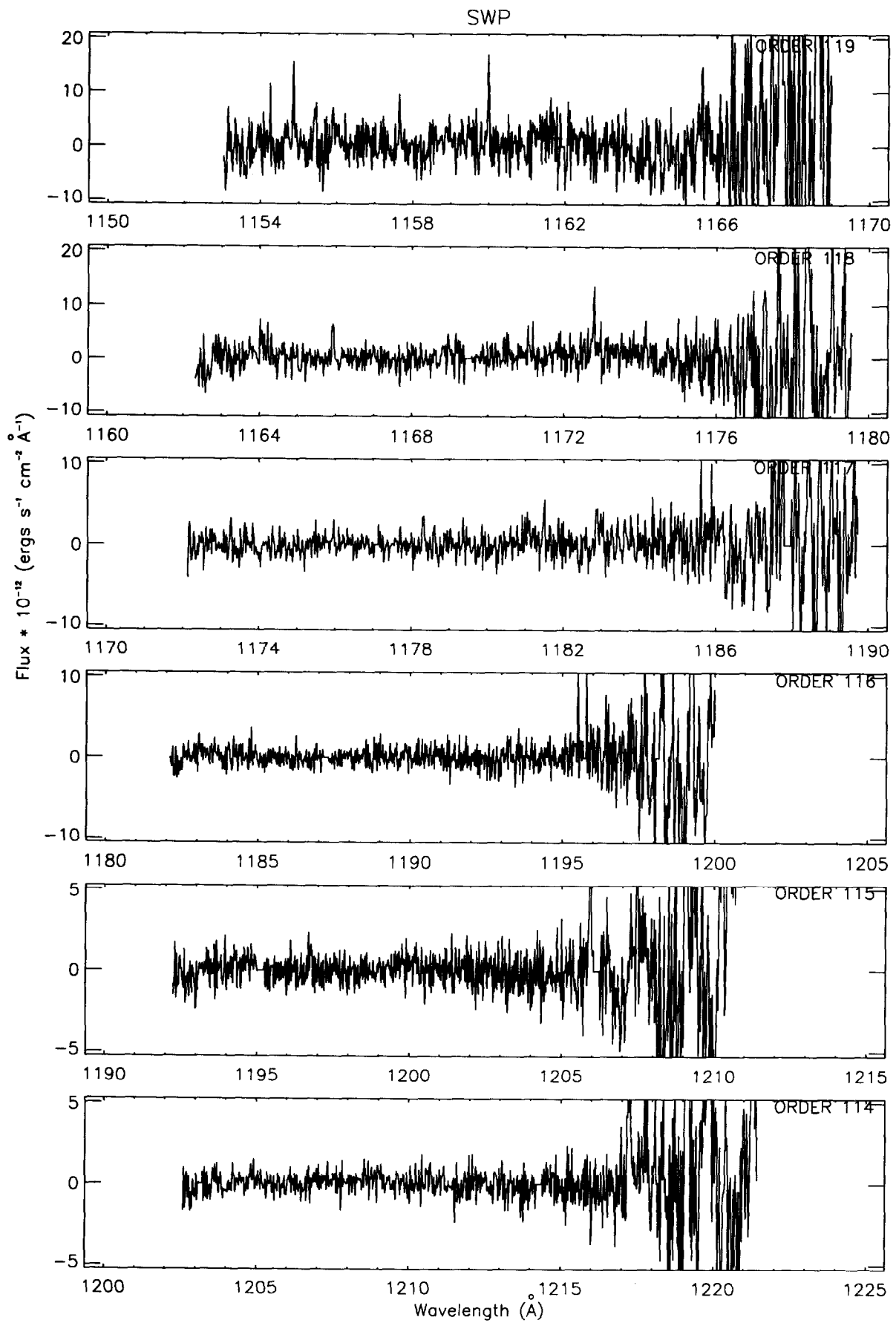
- Bruegman, O.W. & Crenshaw, D.M. 1992, BAAS, 24, 1140
Crenshaw, D.M., Bruegman, O.W., Johnson, R., and Fitzurka, M. 1996, submitted to PASP
Crenshaw, D.M., Bruegman, O.W., & Norman, D.J. 1990, PASP, 102, 463

TABLE 1
IUE High-Dispersion Artifacts

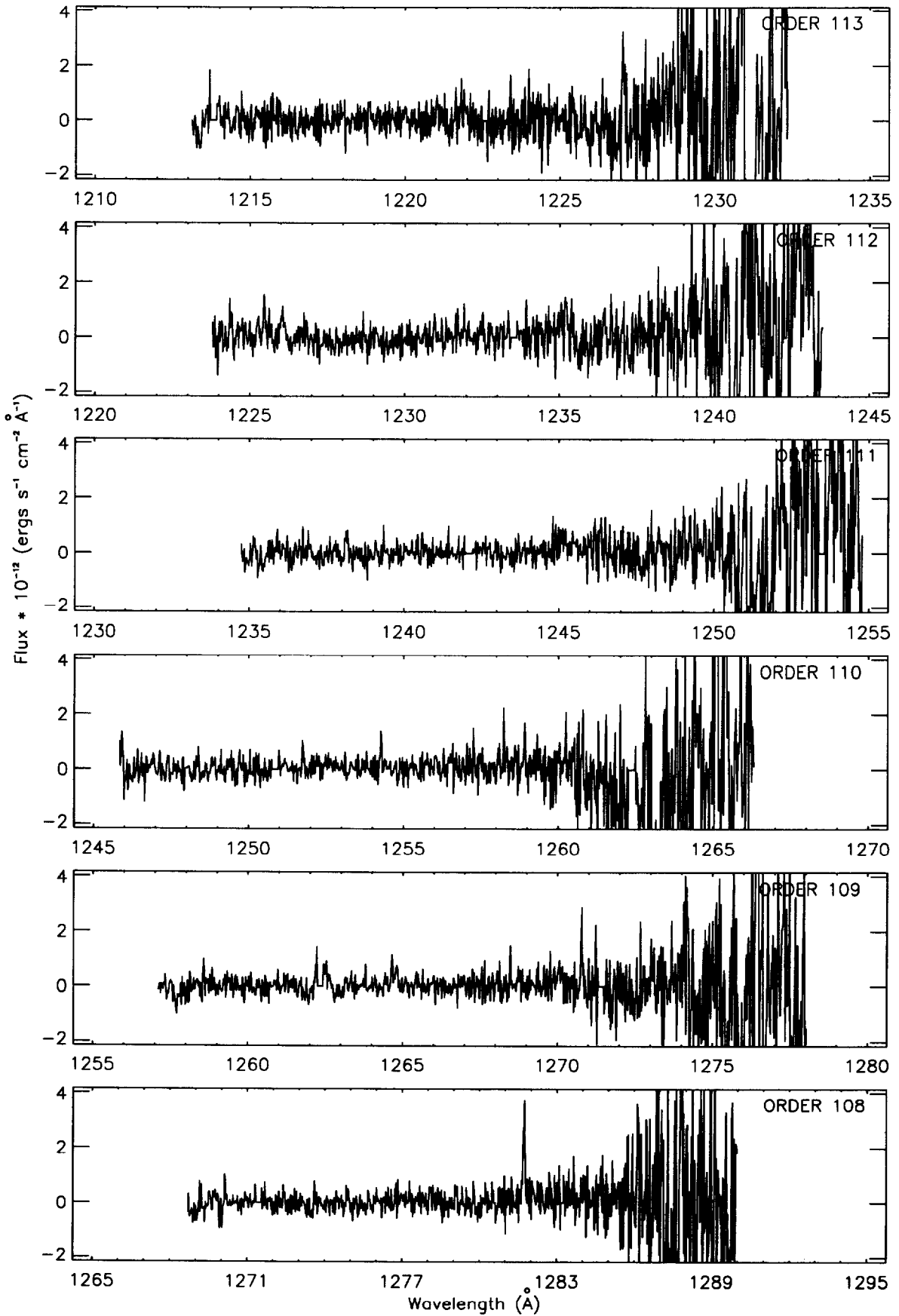
SWP			LWP			LWR		
Order	λ (Å)	F_{λ}^a	Order	λ (Å)	F_{λ}^a	Order	λ (Å)	F_{λ}^a
119	1154.9	16.	93	2483.3	1.1	122	1888.3	25.
119	1160.0	17.	80	2880.4	0.26	112	2067.3	1.4
118	1165.9	6.1				112	2074.4	1.7
118	1172.8	13.				107	2167.1	1.1
116	1195.5	12.				106	2171.7	1.7
116	1195.8	16.				100	2303.2	1.3
115	1205.9	9.6				100	2322.3	0.8
108	1281.7	3.7				94	2450.1	1.5
106	1298.6	1.0				93	2501.1	0.48
104	1320.8	1.0				87	2670.1	0.26
103	1337.8	0.7				86	2694.4	0.23
101	1369.8	1.9				84	2756.2	0.22
95	1453.6	1.7				82	2808.4	0.32
93	1474.3	1.6				82	2829.0	0.28
93	1481.8	1.1				80	2900.6	0.66
93	1483.0	1.6				77	3010.7	0.47
93	1487.7	1.6				76	3029.6	0.46
92	1500.9	1.9				75	3066.4	0.62
92	1504.8	3.0				75	3083.1	0.44
92	1505.5	2.3				75	3100.0	0.62
90	1540.0	3.5				72	3194.3	0.74
89	1549.3	0.9				72	3195.2	1.64
89	1552.0	1.7						
88	1566.5	1.4						
88	1573.0	1.8						
87	1577.9	1.1						
87	1583.9	1.9						
87	1593.2	2.1						
87	1593.5	1.9						
86	1598.5	0.9						
86	1603.6	1.0						
82	1691.1	1.1						
80	1725.9	1.1						
79	1755.5	0.80						
78	1757.7	0.40						
78	1762.4	0.57						
77	1790.1	0.38						
77	1795.5	0.80						
76	1810.1	0.71						
72	1914.3	0.25						
72	1916.0	0.31						
70	1975.0	0.25						
70	1980.6	0.33						
69	2005.0	0.26						
69	2009.5	0.46						
67	2059.1	0.25						
57	2059.5	0.39						

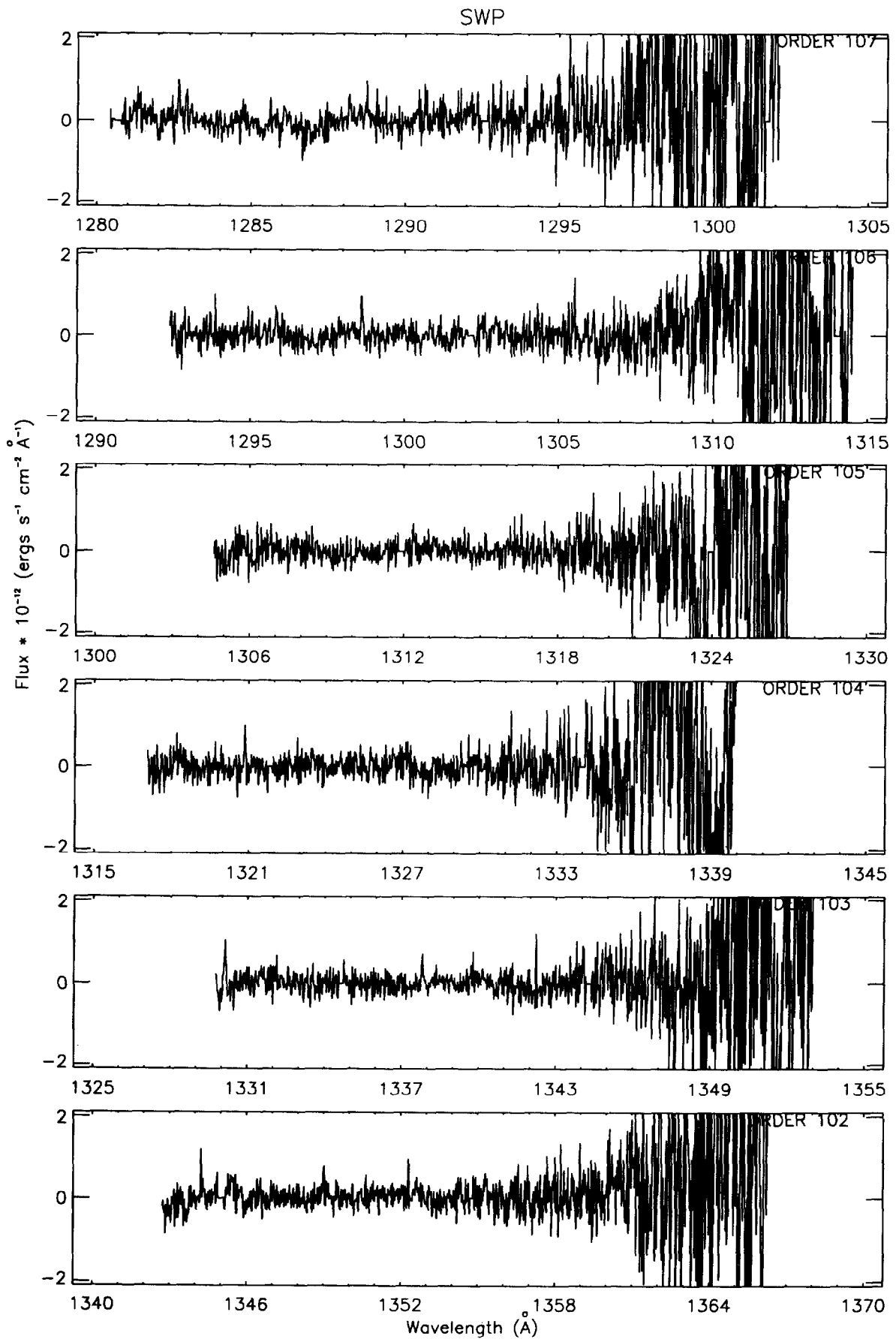
^aFlux at peak in units of 10^{-12} ergs s^{-1} cm^{-2} Å^{-1} .

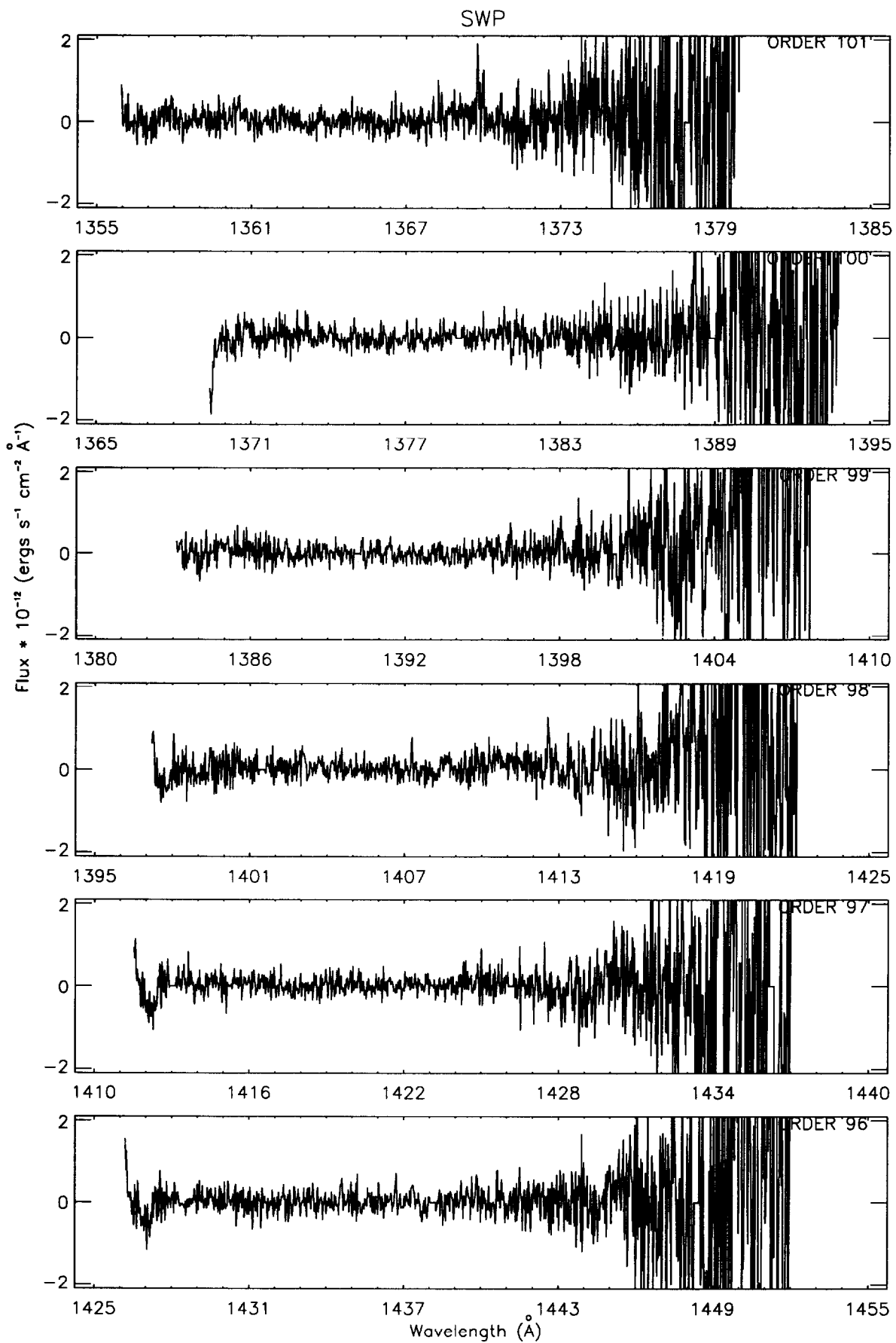


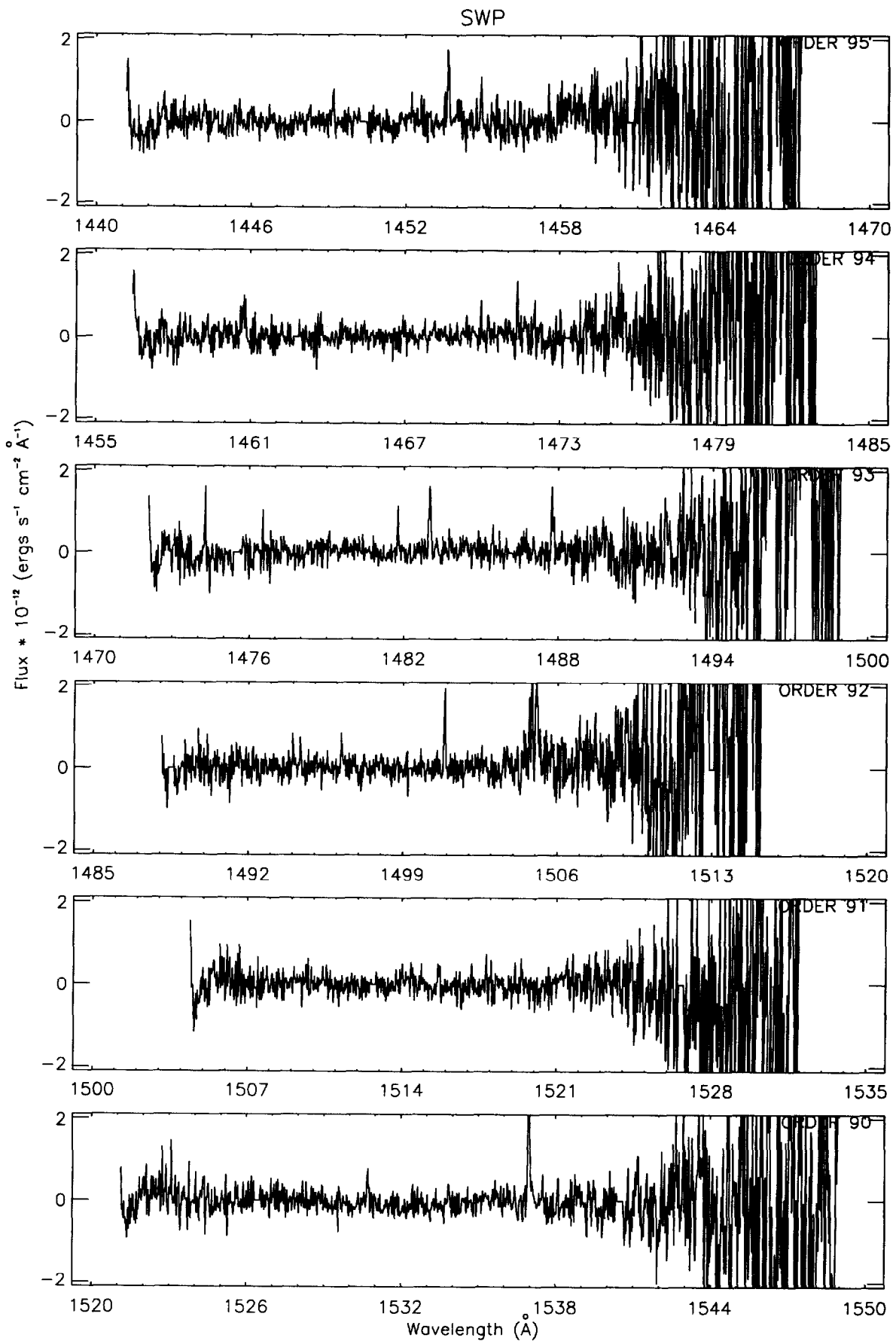


SWP

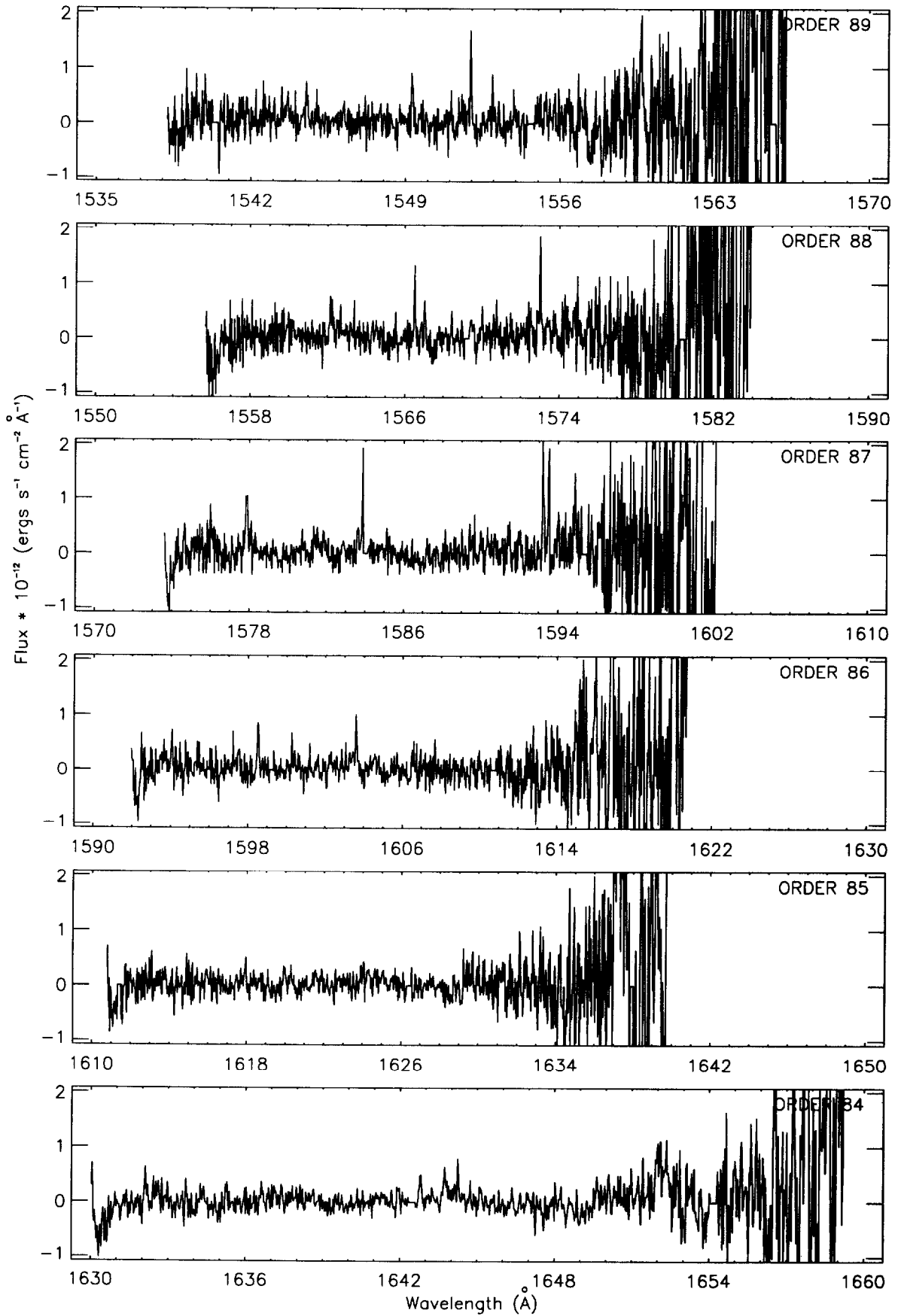




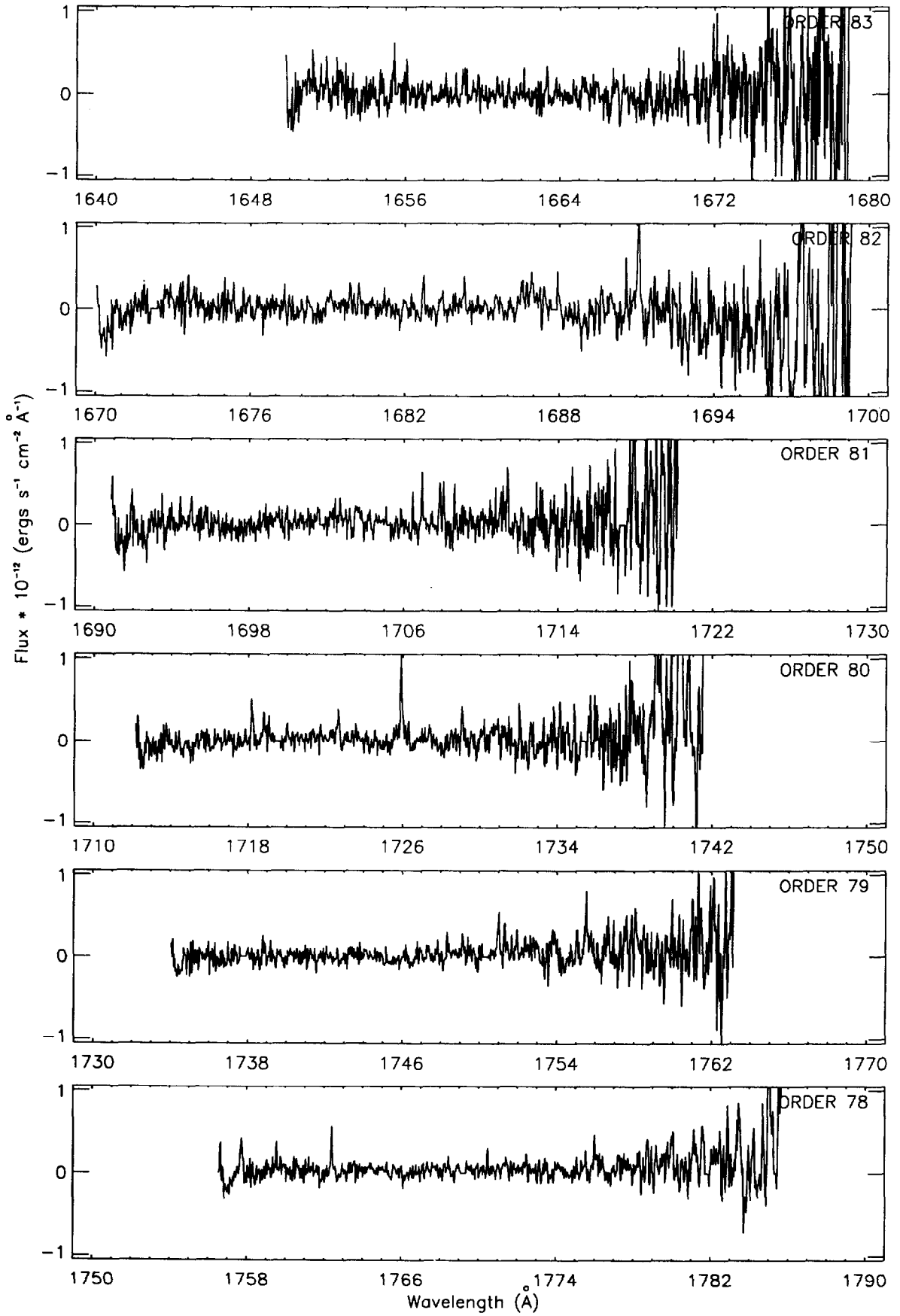


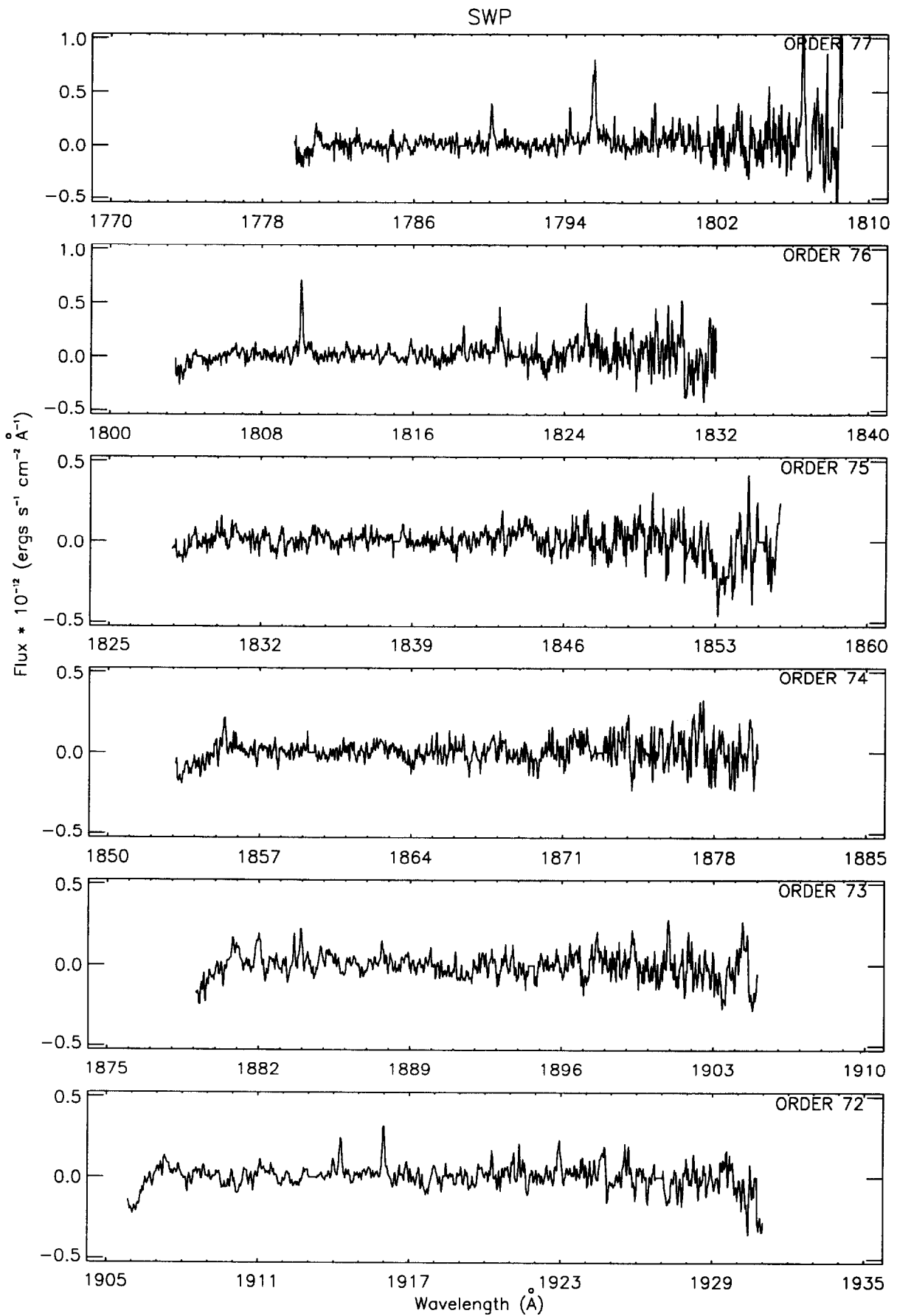


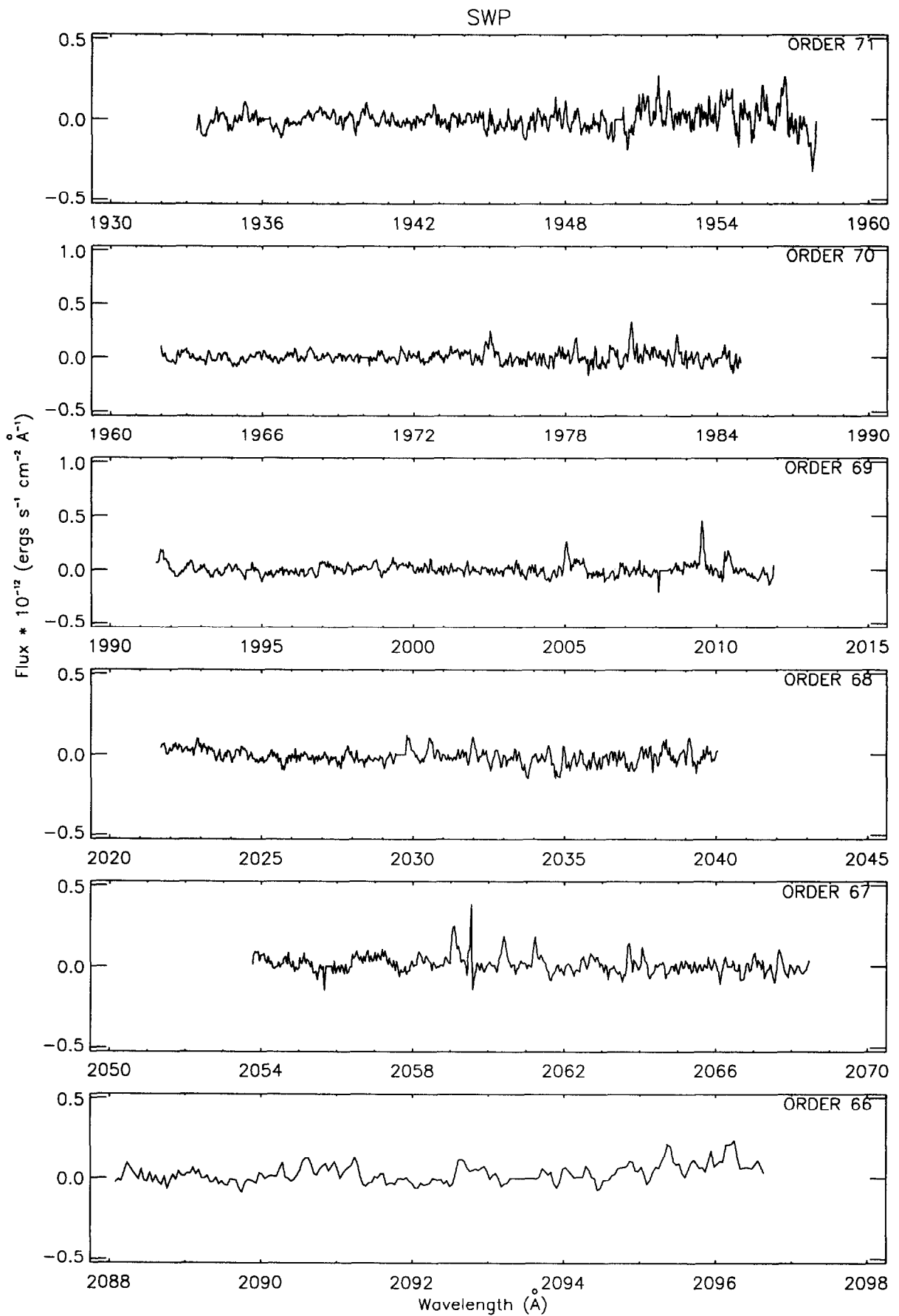
SWP

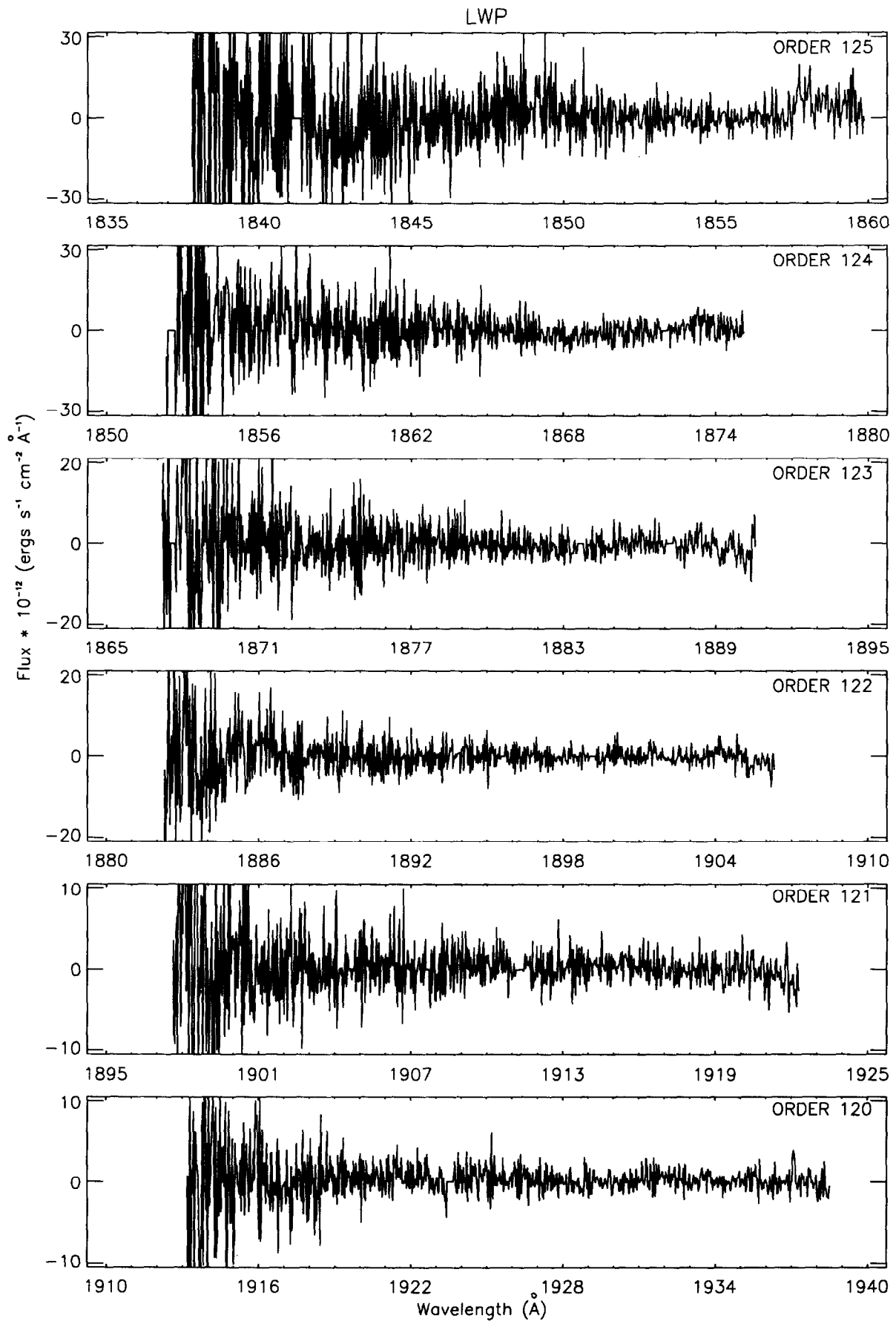


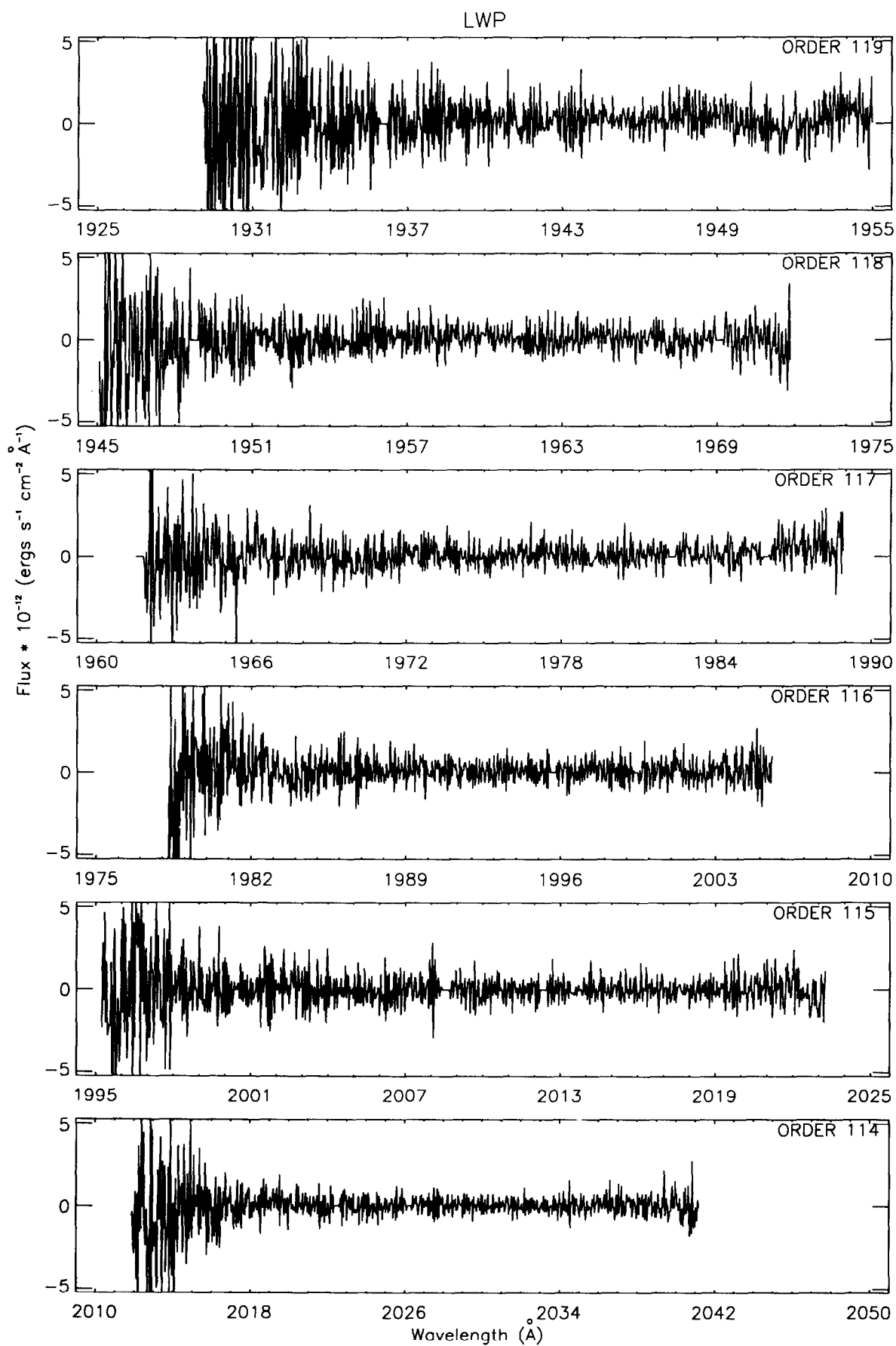
SWP

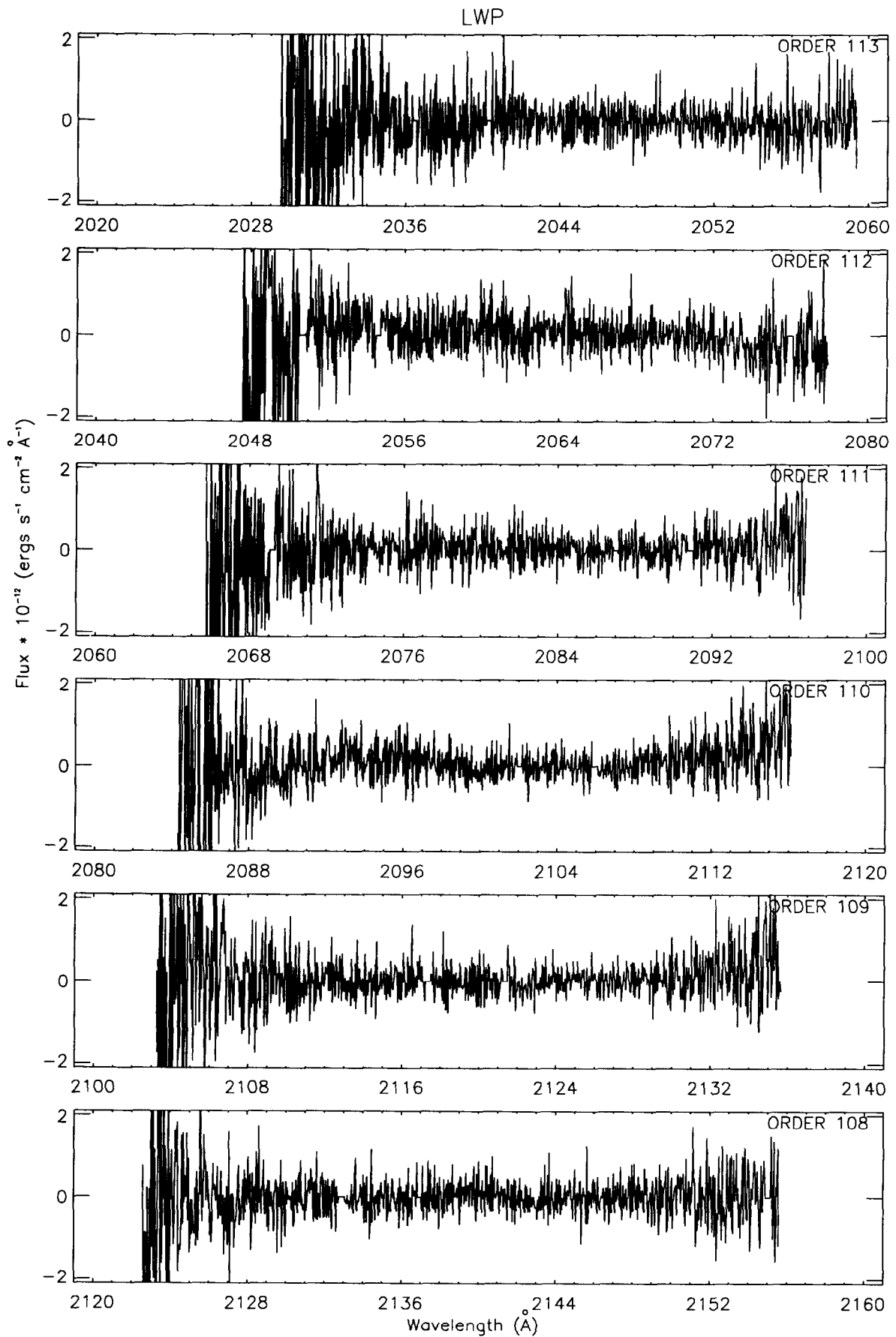


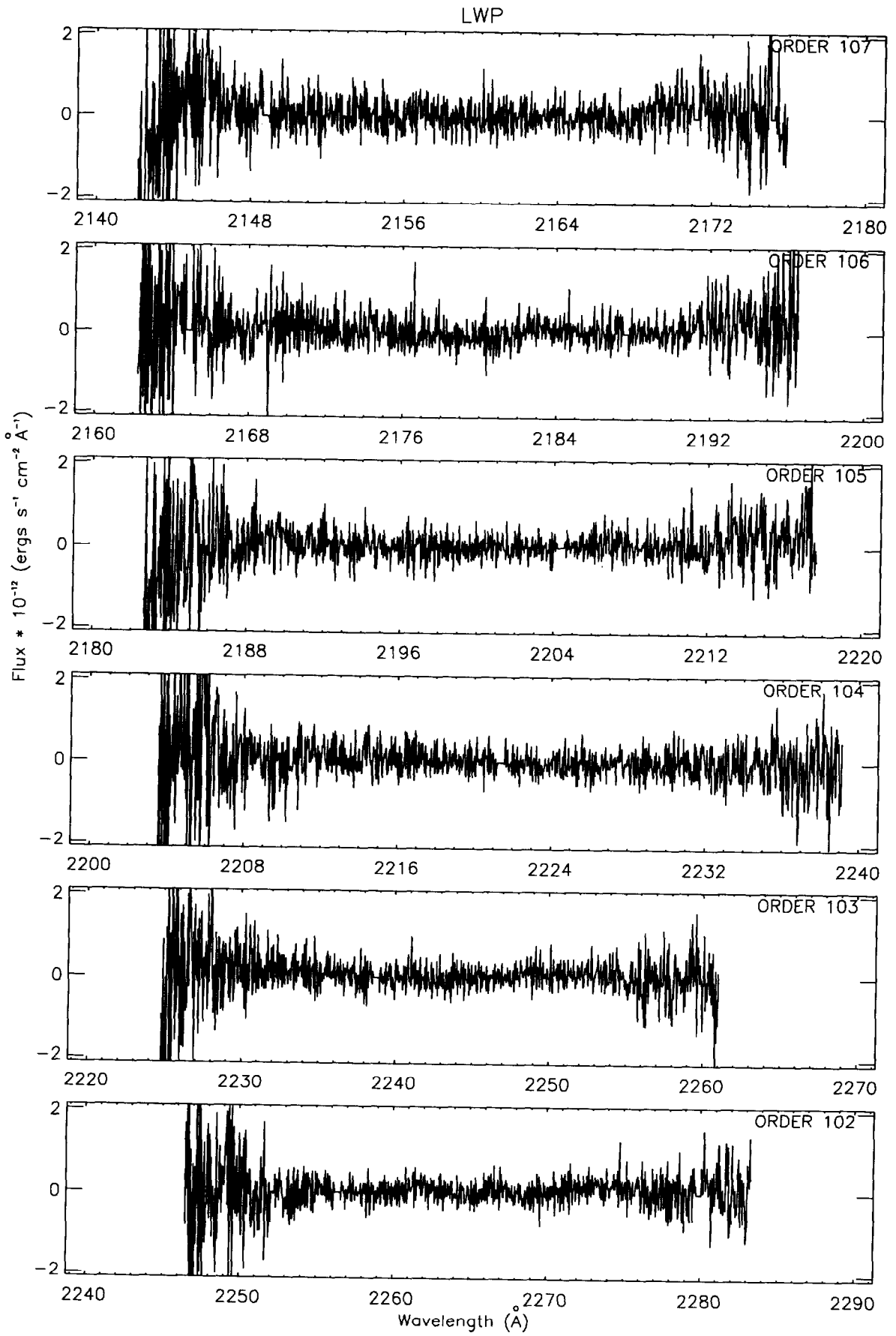


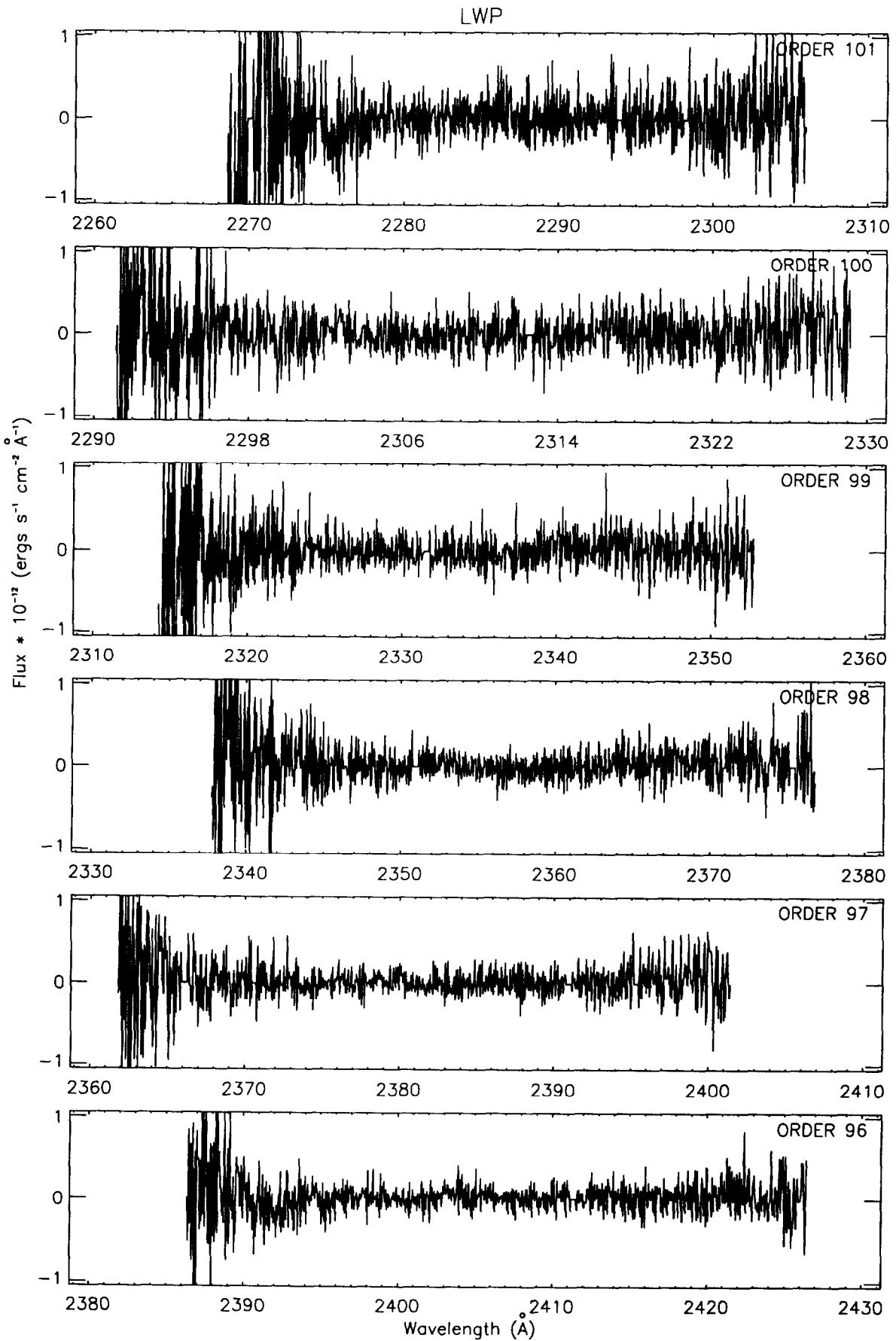


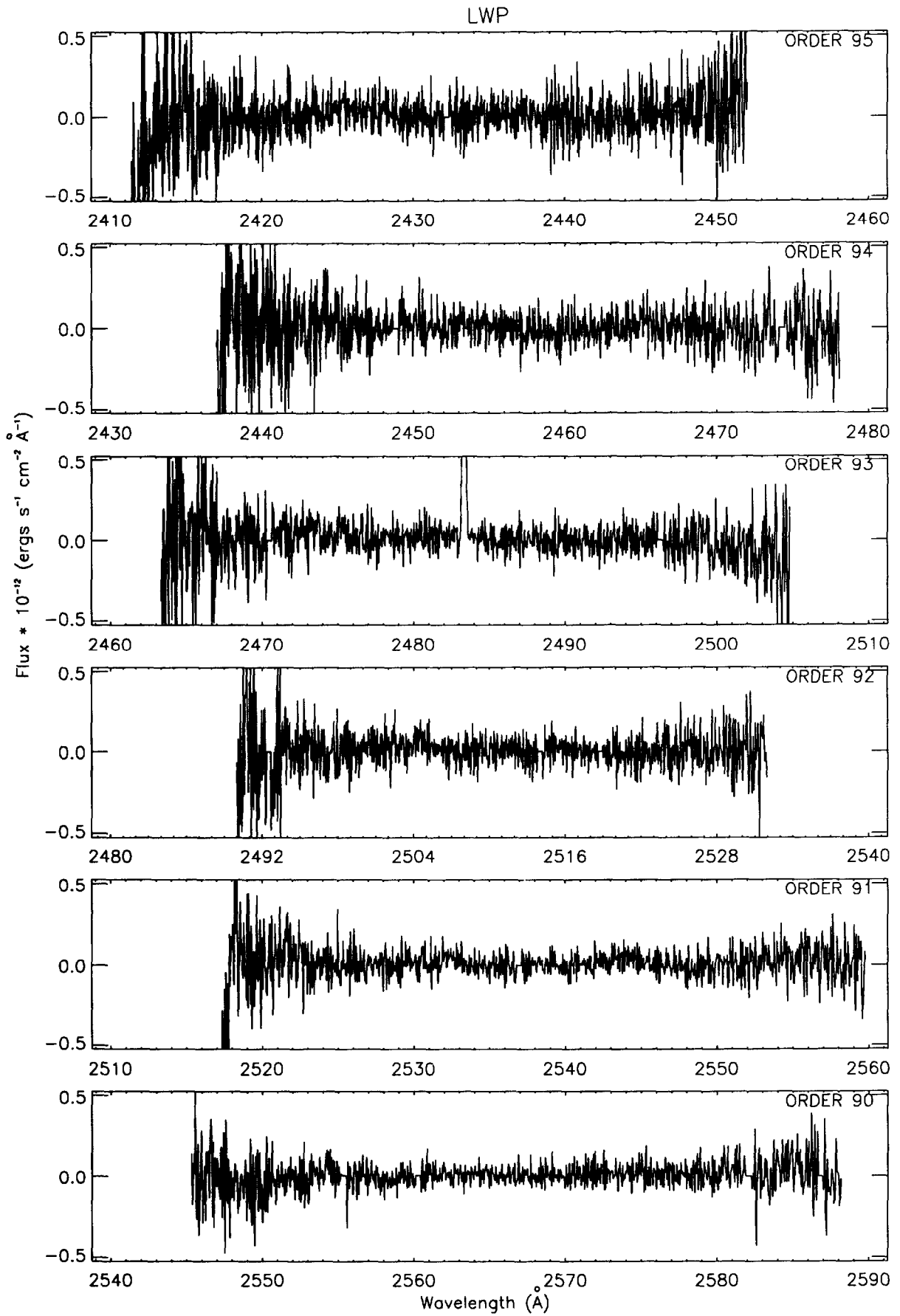


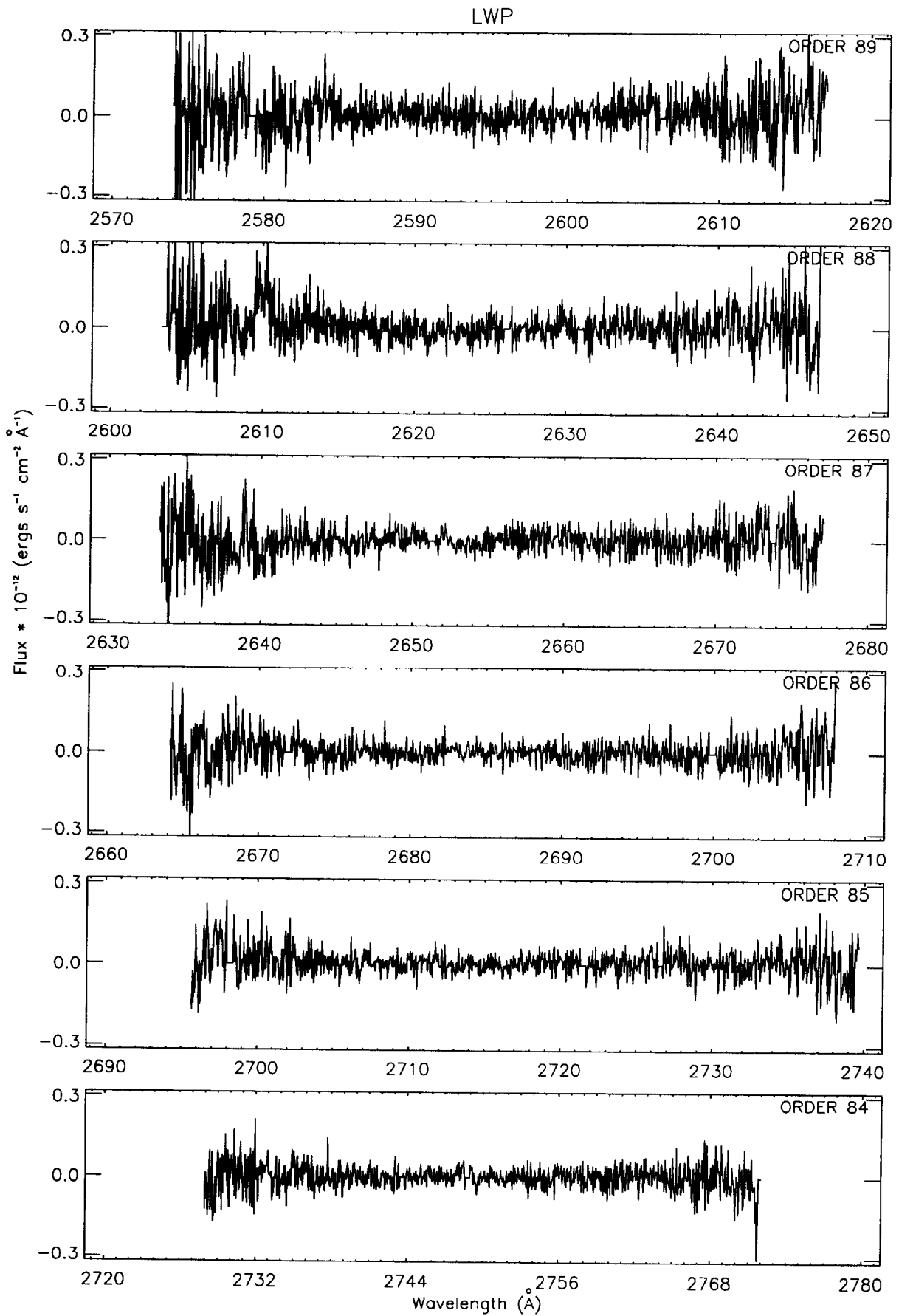


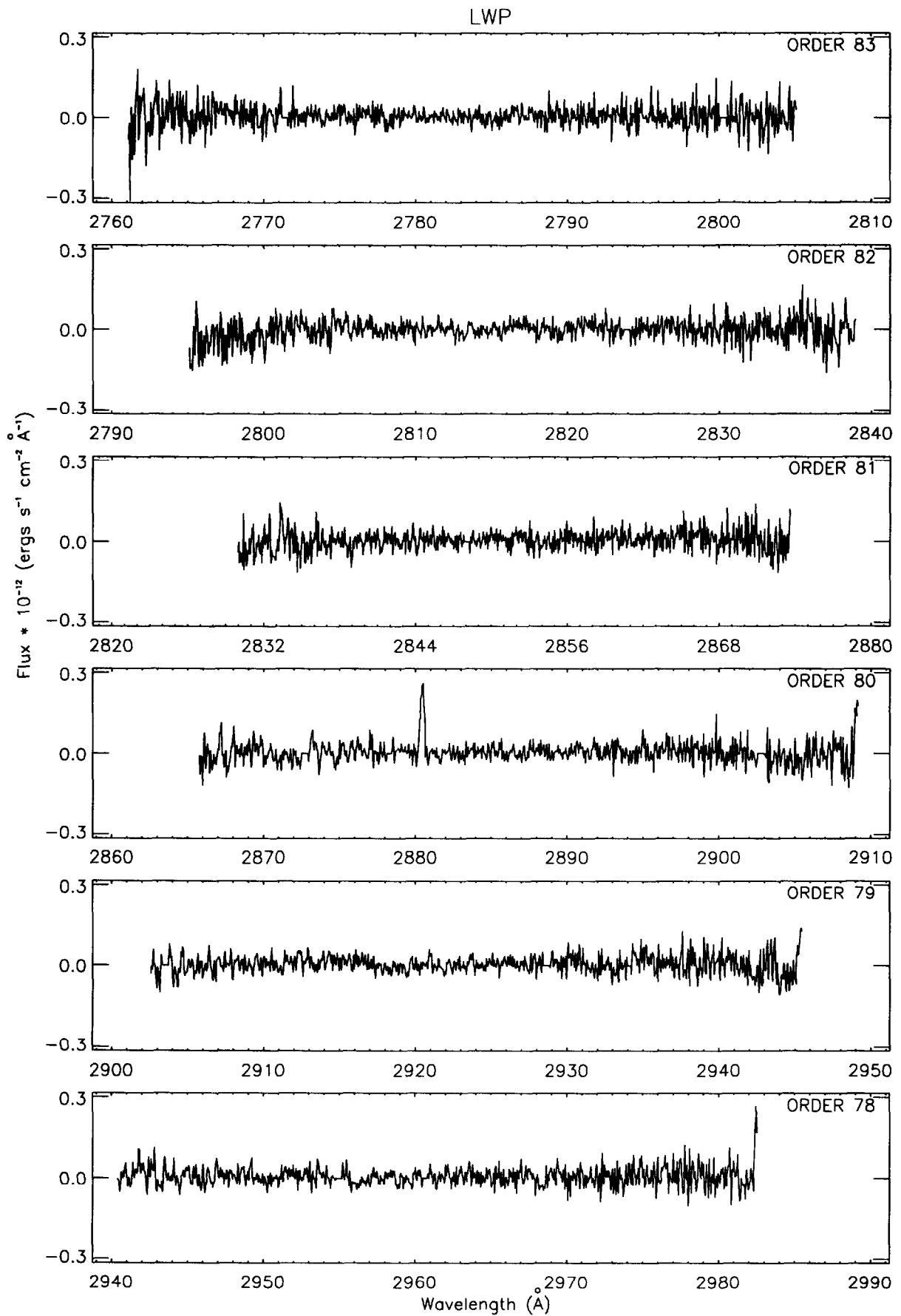


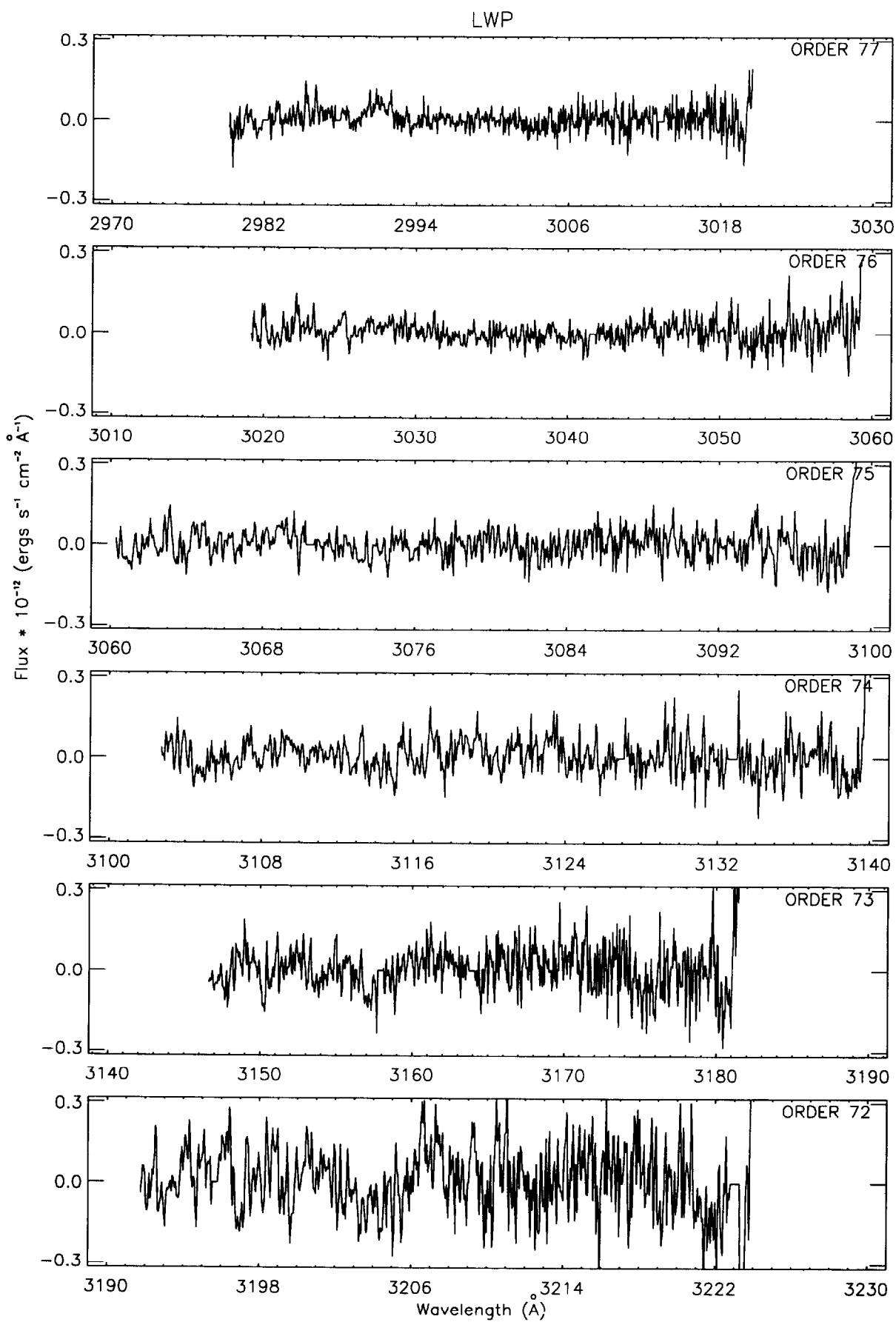


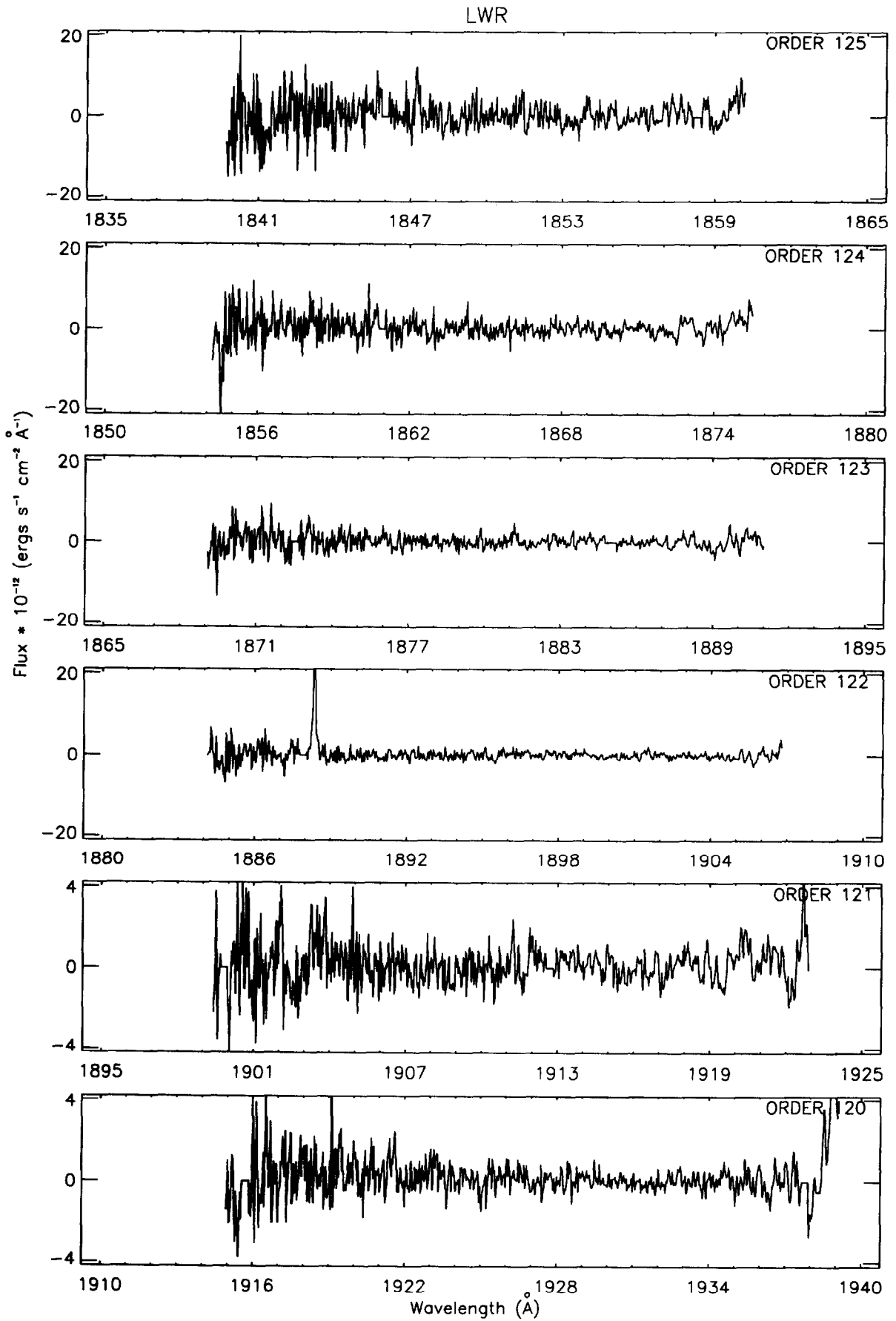


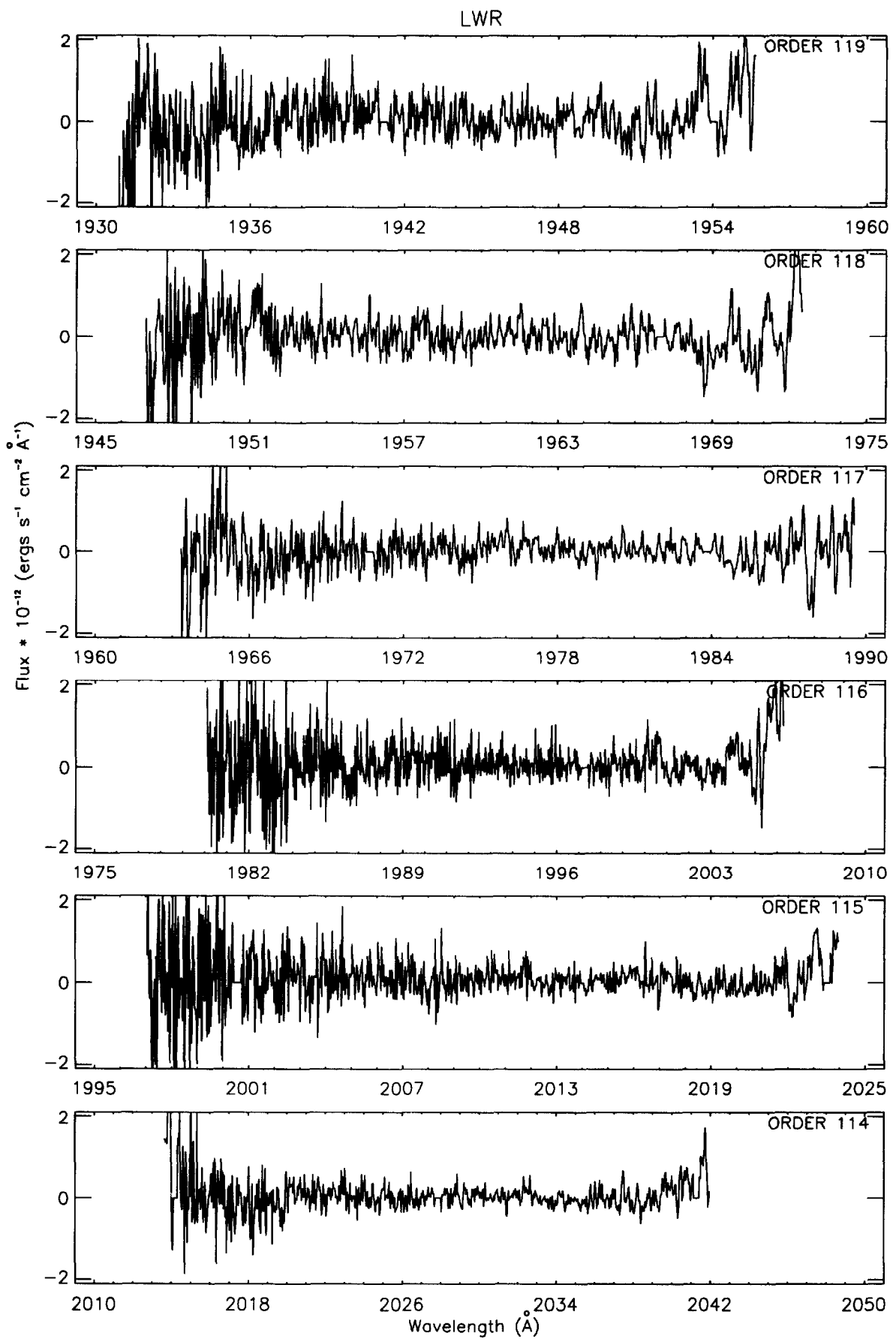


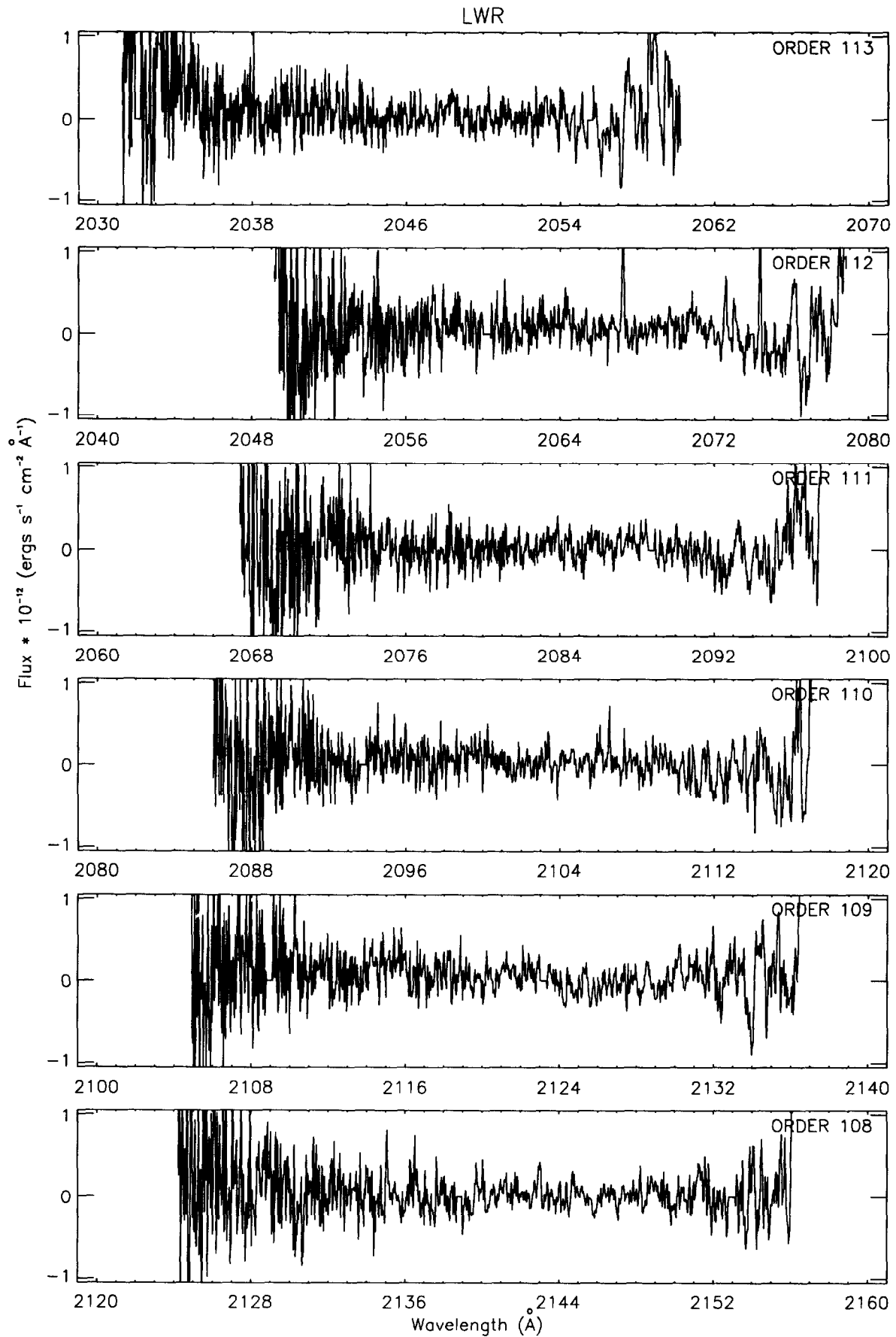




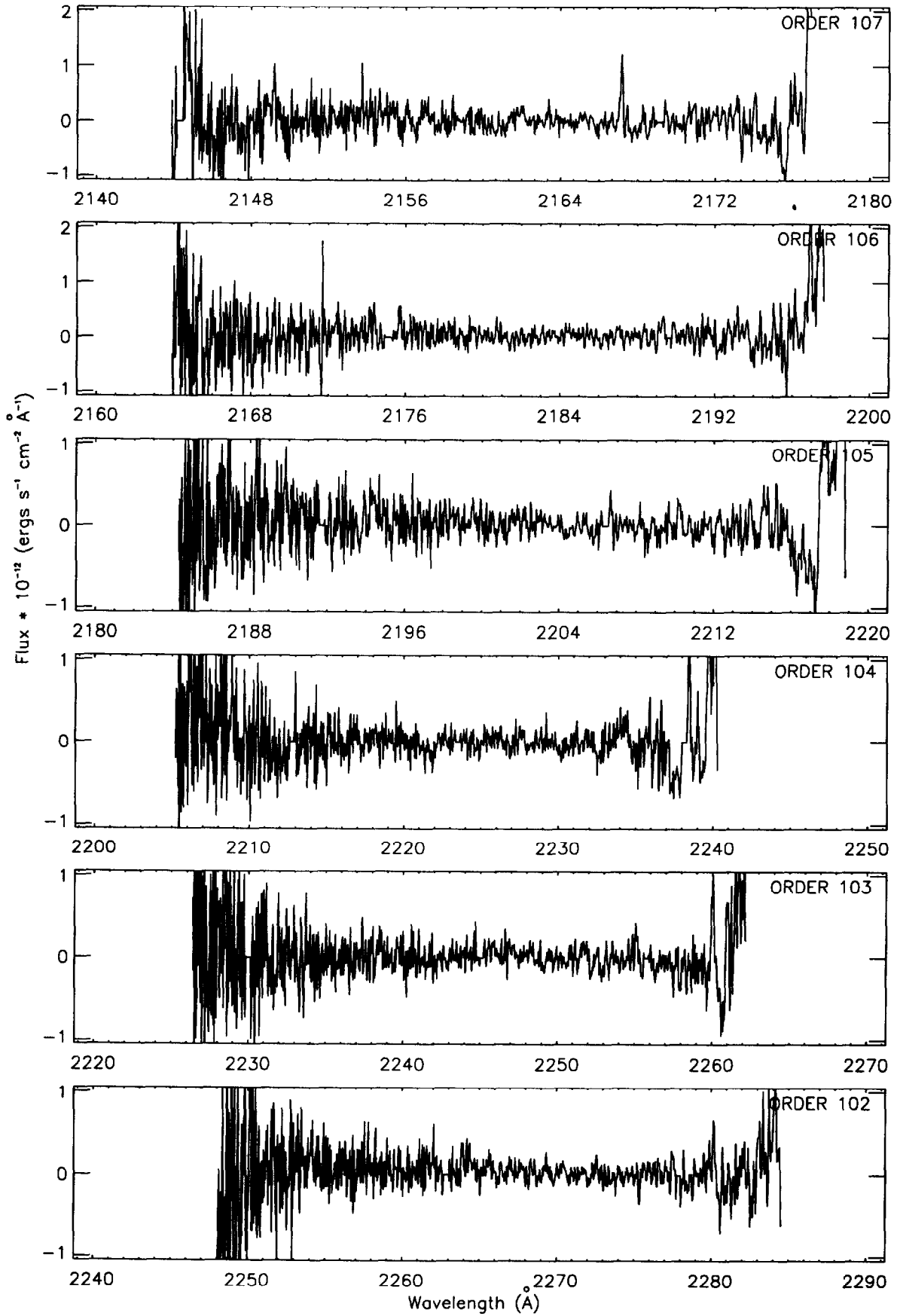


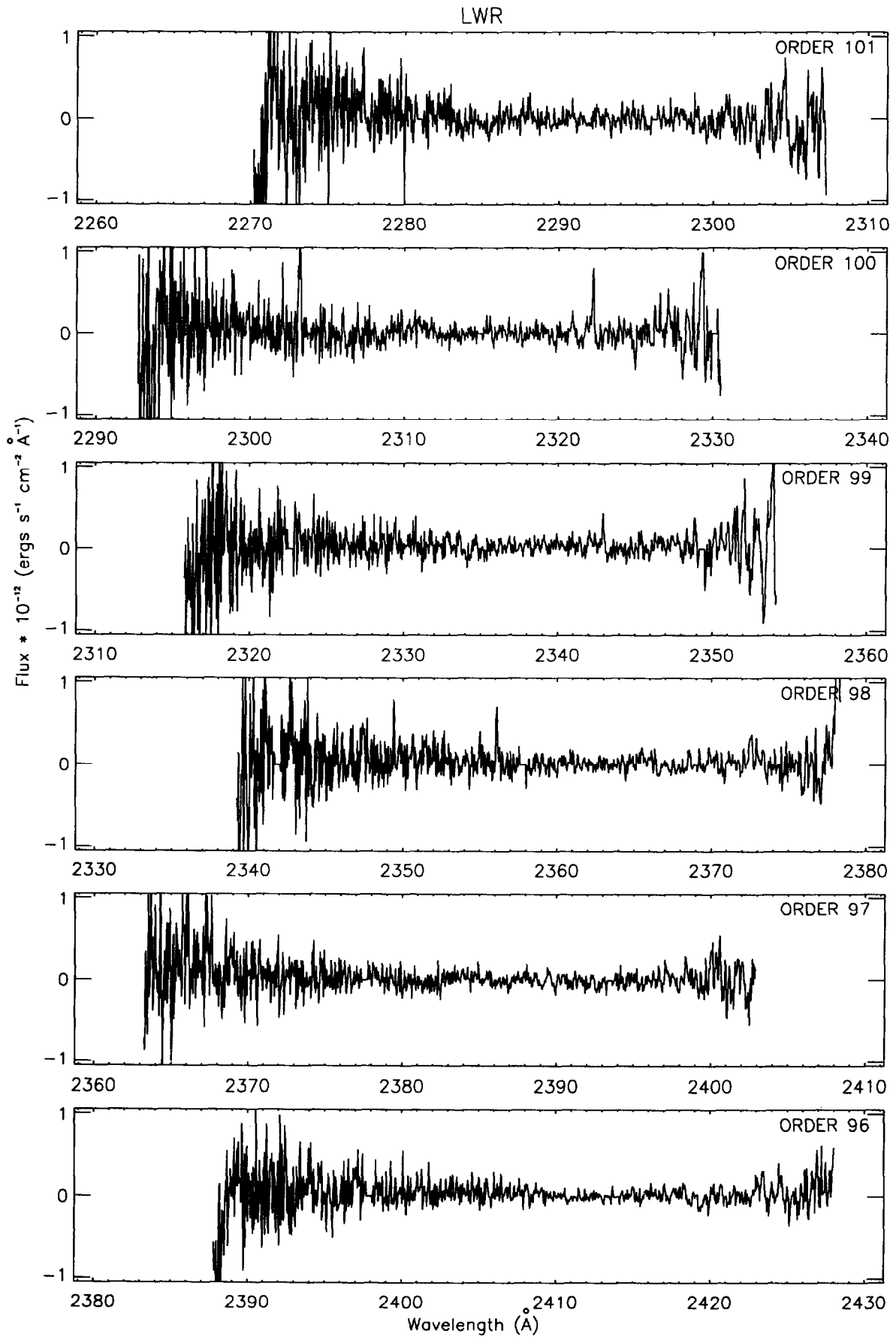




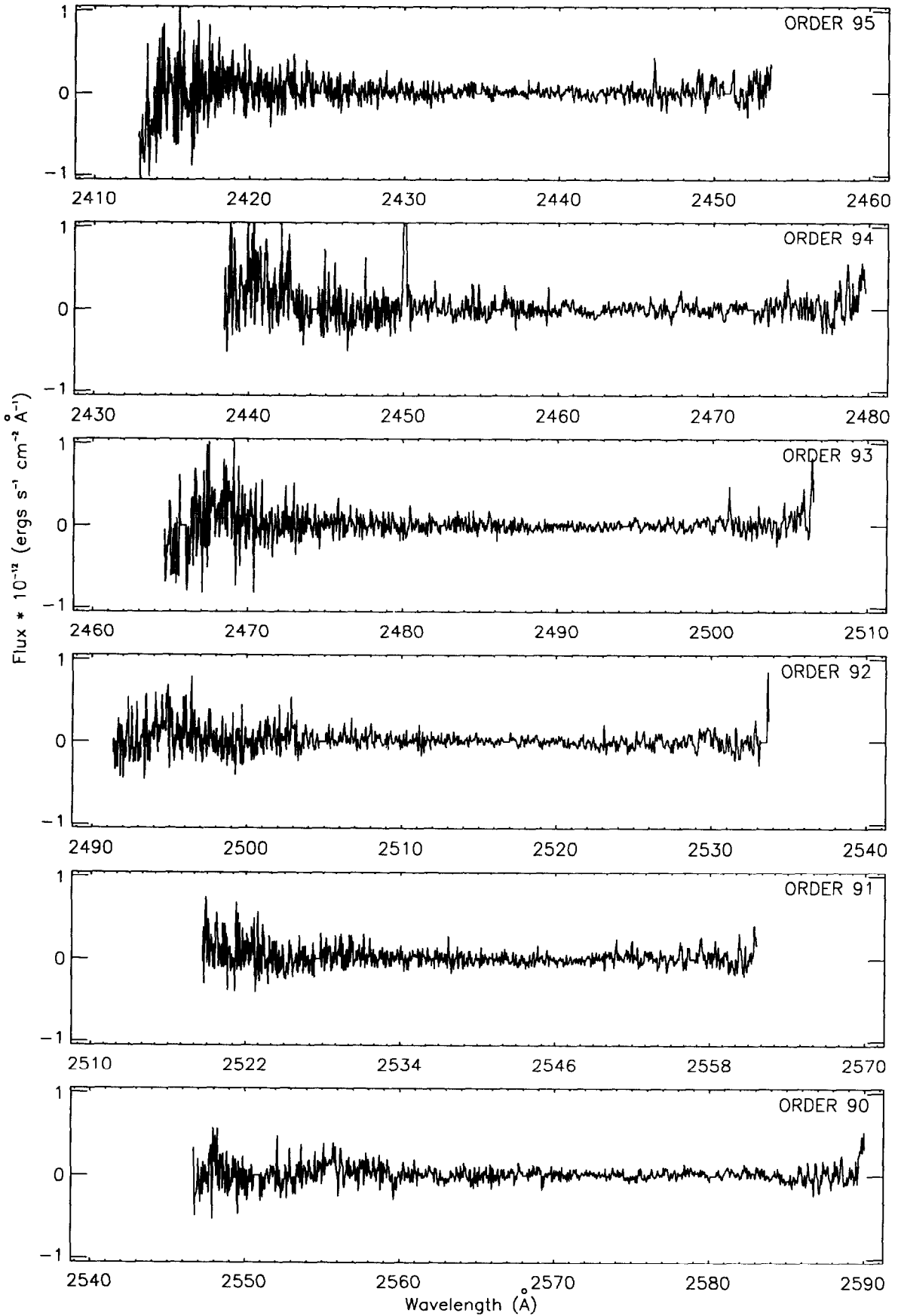


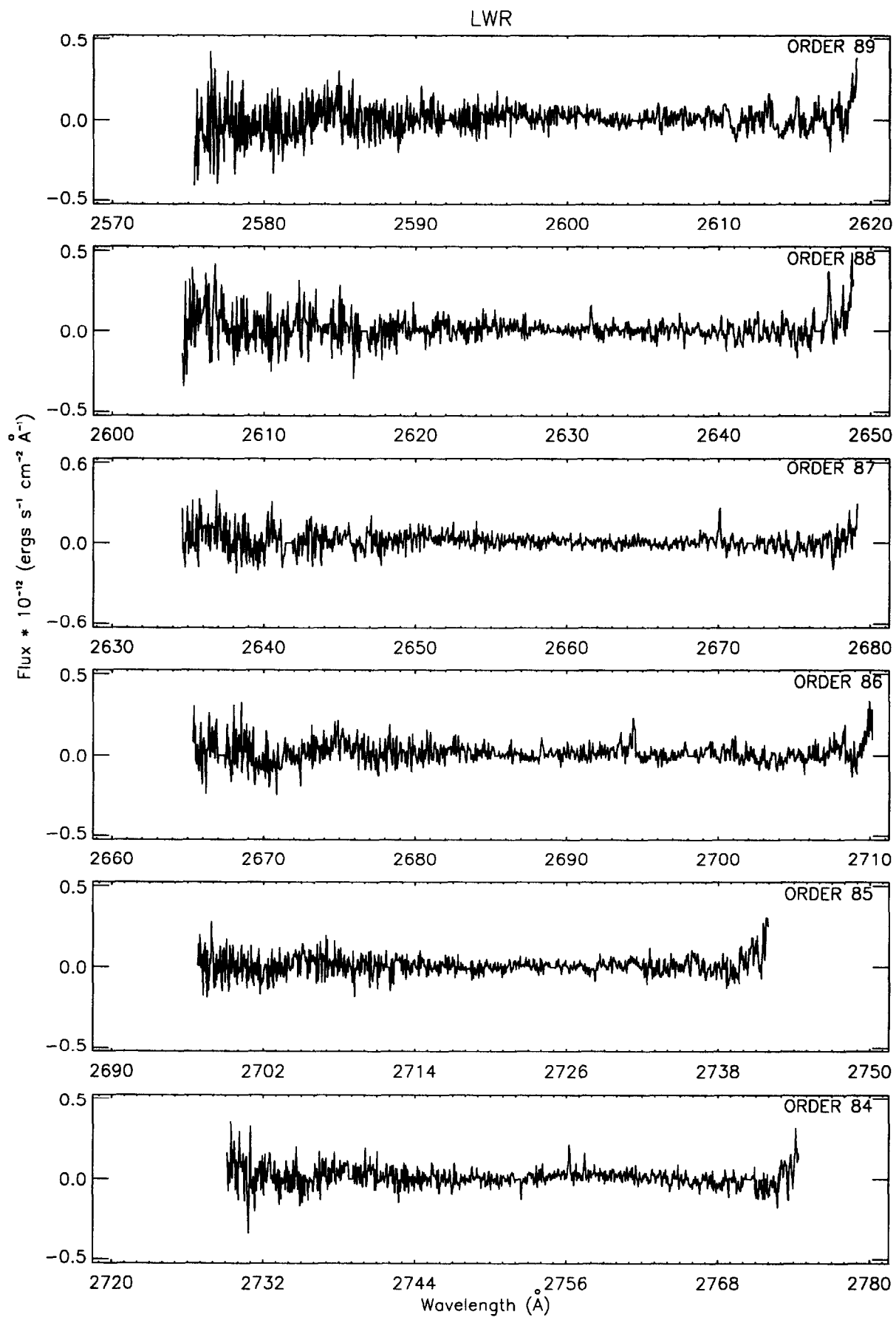
LWR

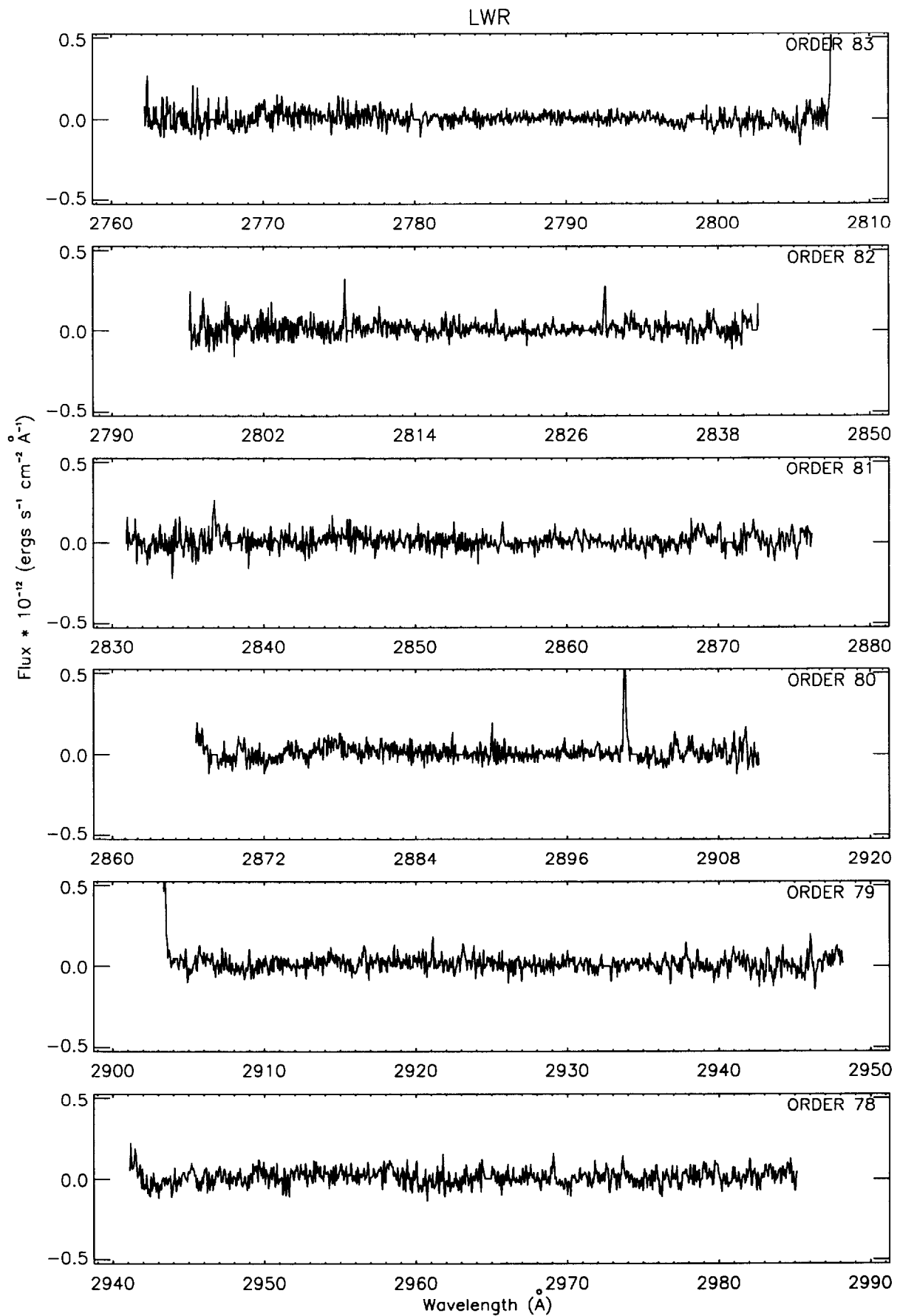




LWR







LWR

